



ISSN 2314-5609
Nuclear Sciences Scientific Journal
6, 35-53
2017
<http://www.ssnma.com>

GEOLOGY AND GEOCHEMISTRY OF THE PERALUMINOUS GRANITES AT WADI UM ADDEBAA AREA, SOUTHEASTERN DESERT, EGYPT

FARRAGE M. KHALEAL

Nuclear Materials Authority, P. O. Box 530 El Maadi, Cairo, Egypt

ABSTRACT

Wadi Um Addebaa area is located about 70 km Southwest of Marsa Alam City. The rocks exposed in this area include: ophiolitic metagabbro, ophiolitic mélange, peraluminous granite and post granite dykes and veins. The most common feature in the studied peraluminous granite is the presence of spessartine garnet aligned in monomineralic bands within its periphery (1m thick) along the contact with the surrounding ophiolitic schists.

Petrographically, the peraluminous granite is mainly composed of sodic plagioclase (An 5-15), K-feldspar, quartz, muscovite and biotite. Sericite and chlorite are secondary minerals. Tourmaline, spessartine, zircon, allanite and opaques are accessory minerals.

Geochemical characteristics of the studied peraluminous granite indicate that this granite crystallized from relatively soda rich magma having peraluminous character, I-type, Syn-collision setting and has calc-alkaline affinity. It is emplaced at relatively shallower depth (water pressure 3-2 kb) in the crust and crystallized at temperature ranges from 800 to 760°C. It possesses high content of LILE (Rb, Y & Zr) and has a moderate to high content of HFSE (Cu, Zn, Pb, As, Bi & W). It constitutes an average 6.7 ppm of Be content. Accordingly, it is believed that this granite is the source of beryl mineralization in Wadi El Gemal area.

Microprobe study of garnet revealed spessartine composition with core rich in CaO, MgO, TiO₂ and Y₂O₃, while the rim is enriched in FeO, Al₂O₃ and SiO₂. MnO shows variable enrichments. The composition differs due to the variation in the ratio of Fe and Mn. Whereas the Mn increases in the core more than the rim whereas Fe vice versa.

Radiometric study shows that, the peraluminous granite shows uranium and thorium contents with averages of 19 ppm and 4.5 respectively, suggesting that it is fertile granite.

INTRODUCTION

Wadi Um Addebaa is located about 70 km southwest of Marsa Alam City on the Red Sea coastal plane. It is a tributary of W. El Gemal. The studied Peraluminous granite is exposed in different locations in Wadi El Gemal area (W. Um Solimat, W. Sikait, W. Um El Kheran, W. Um Baanib and W. Um Addebaa). Among them, Peraluminous granite of W. Um Addebaa area comprises garnet crystals,

in the periphery, organizing in clear bands

Peraluminous granites constitute a chemical subdivision of the granite family in which the whole rock molar ratio of alumina to lime, soda and potash [$Al_2O_3/(CaO+Na_2O+K_2O)$] abbreviated A/CNK is greater than unity. Owing to their chemical and mineralogical similarities to metapelites, peraluminous granites are often considered to be genetically linked with these metasediments as source

rocks and are thus referred to S-type granites. Peraluminous leucogranites are commonly associated with regionally metamorphosed and highly folded belts containing pelitic and quartzo-feldspathic sediments, for example the Tasman mobile belt of eastern Australia (Phillips, 1981).

Collisional leucogranites are characterized by peraluminous compositions and very low concentrations of CaO, MgO & FeO. In leucogranites, muscovite is a characteristic mineral, along with tourmaline or biotite. Almandine-spessartine garnet and minor sillimanite can also occur. Tourmaline and biotite are often exclusive of each other (Nabelek et al., 2001)

Syn-collision peraluminous granitic segregations are commonly associated with regionally metamorphosed terrains (Clemens and Wall; 1981); Debonet. al.,(1986); Inger and Harris (1993); Ibrahim et. al., (2001); and Salehet. al., (2002). Numerous mechanisms have been proposed to explain the derivation of these segregations from the metamorphosed host rock, but partial melting of metapelites (Barbey, 1990) is still the most widely accepted model for the generation of these peraluminous leucogranites. Most of water required for this partial melting process may be derived from the breakdown of hydrous silicates in these pelites such as muscovite and biotite minerals (Fyfe, 1969).

Peraluminous granites with near-eutectic composition are common in collisional orogens, where they were produced by partial melting of deformed and metamorphosed accretionally-wedge and ocean-floor sediments. Whilst there is a general agreement that leucogranites are anatectic of pelitic crustal sources. The heat sources for their production have remained controversial (Royden, 1993 and Thomposon and Connolly, 1995).

The pegmatitic granite is characterized by low contents of REEs = (18 – 51 ppm). The particularly low $[La/Yb]_n$ ratio in the garnetiferous granite is due to fractionation of

LREE-rich phases such as monazite, allanite and apatite (Mohamed and Hassanen (1997). Alternatively, the low $[La/Yb]_n$ ratio in the garnetiferous granite is due to the light garnet abundance which appreciably accommodated the HREE (Gronet and Silver (1983)). Most of Egyptian granites are mainly metaluminous to slightly peraluminous, except rare ones (G. El-Sella and G. Ribdab), associated with U-mineralization (Ibrahim et. al., 2001).

In Egypt peraluminous leucogranites represent phases of late orogenic to an orogenic granite complex. They brought about Mo, Sn, W, U, and Nb-Ta mineralization in the form of stock works or in the quartz veins within the granitic rocks (Hassan et al., 1984, Takla and Nowier 1980).

The main target of the present work is to study the geology, geochemical characteristics and radiometry of the peraluminous granite embracing nice garnet crystals at Um Addebaa area, SED, Egypt.

METHODS OF STUDY

For petrographic and mineralogical study, nine polished thin sections were prepared at the University of New Brunswick (UNB), Canada. Complete chemical analyses (major, trace and REE elements) for nine samples of the studied peraluminous granite were carried out by using X-ray Fluorescence spectrometer at Activation Laboratories (ACT-LABS), Ontario, Canada. Backscattered electron images were collected by scanning electron microscope-energy dispersive spectrometry (BSE) (model JEOL 6400 SEM) at the Microscopy and Microanalyses Facility, University of New Brunswick (UNB), Fredericton, New Brunswick, Canada.

GEOLOGICAL SETTING

Wadi Um Addebaa area is located at ~70 km SW of Marsa Alam City. It is accessible after 52 km to the south through the Red Sea Highway and then 32km to the west through W. El Gemal. Wadi Um Addebaa intersected

with W. El Gemal at the point 24°34'14"N and 34°53'26"E. The peraluminous granite is well exposed within W. Um Addebaa at the intersection 24°34'31"N and 34°53'38"E.

The rocks exposed in Um Addebaa area (Fig.1) include: ophiolitic metagabbro (oldest), ophiolitic mélange, peraluminous granite and post granite dykes andveins (youngest).

The general geology of this area was described by many authors (Hume, 1934; Omar, 2001, Mahmoud, 2009 and Khaleal and Mahmoud 2009).

The Ophiolitic Metagabbro

The metagabbro is in mountain size and characterized by dark green color and medium to coarse grained. The metagabbro is thrust over the ophiolitic mélange.

The Ophiolitic Mélange

The ophiolitic mélange composed of ophiolitic fragments of variable sizes comprising of serpentinites and metagabbro embedded in mélange matrix mainly of different varieties of schists (tourmaline-garnetiferous- biotites-chists). Petrographically, they are composed mainly of quartz, plagioclase and biotite.

Muscovite and chlorite are secondary minerals. Apatite, zircon and garnet are accessory minerals. They are similar to those in Nugrus–Sikait area described by Saleh (1997). Serpentinites are commonly altered into talc carbonates of creamy color. They are characterized by their cavernous nature. Sometimes instead of talc carbonates, the serpentinites are altered to talc-tremolite rock containing megascopic tourmaline (Fig.2).

The Peraluminous Granites

The peraluminous granites exposed as small bosses and dyke-like body (< 1.0 km²) intruding the ophiolitic mélange at the middle part of the mapped area causing truncate the foliation of the schist at high angles. It is emplaced along N-S trend, about 250 m long and 60 m in width. The peraluminous granites are medium to coarse-grained or even pegmatitic and white in color forming mass of low relief (Fig. 3) with sharp intrusive contacts against the ophiolitic mélange. They are deformed and show well-known spheroidal weathering. The periphery, about 1m wide, of the studied peraluminous granite is characterized by presence of monomineralic bands of visible spessartine garnet (Fig. 4a&b).

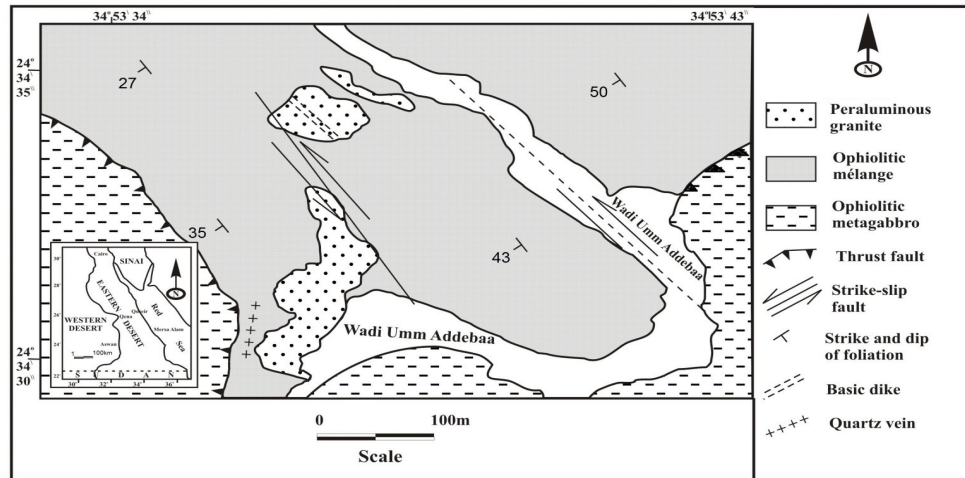


Fig. 1: Geologic map of Um Addebaa area, SED, Egypt (Modified after Mahmoud 2009)



Fig. 2: Close-up view showing serpentinites altered to talc-tremolite rock containing megascopic tourmaline at W. Um Addebaa, SED, Egypt



Fig. 3: Dike-like body of the peraluminous granite at W. Um Addebaa, SED, Egypt. Camera looking NNW

PETROGRAPHY

The peraluminous granites are medium to coarse-grained and mainly composed of K-feldspar, sodic plagioclase (An 5-15), quartz, muscovite and biotite. Sericite and chlorite are secondary minerals. Tourmaline, zircon, allanite and garnet are common as accessory minerals. Myrmekitic texture is common. The presence of myrmekitic texture represents strong evidence for metasomatic origin, which are common in magmatic granite (Smith, 1974). Myrmekitic texture was formed due to the action of metasomatic processes with the exsolution around the margins of feldspar phenocrysts (Ashworth, 1979). **Garnet**; occurs as large oriented irregular crystals (Fig. 5) with pale pinkish color in plane polarized light, which appears in cracked or skeletal form (Fig. 6). The presence of muscovite as flakes reflects the peraluminous nature of these granites. The presence of two feldspars suggests that the peraluminous granites are mostly subsolvus and crystallized under high water pressure (Greenberge, 1981 and Deer et al., 1992). Locally, the granites are deformed and showing deformational features such as bent plagioclase lamellae, distorted microcline twinning, twisting of mica flakes, strongly undulatory quartz development of myrmekite and recrystallization of feldspars into fine-grained aggregates. All these features point to subsolidus deformation (Pater-

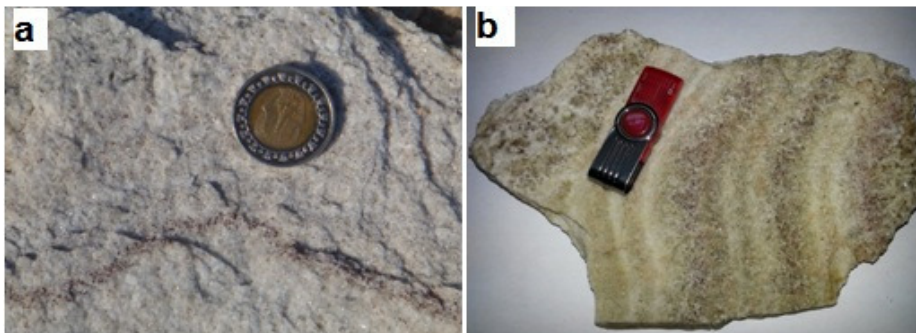


Fig. 4 (a&b): Photos show monomineralic bands of garnet at the periphery of the peraluminous granite, Um Addebaa area, SED, Egypt



Fig. 5: Photomicrograph showing garnet crystals and muscovite in peraluminous granite in Um Addebaa area, SED, Egypt



Fig. 6: Photomicrograph showing cracked crystal of spessartine in peraluminous granite, Um Addebaa area, SED, Egypt

son et al., 1989). Such deformation should be the result of extensive regional thrusting (Greiling et al., 1987), to which the area had been subjected.

The Post granite dykes and veins include basic dikes and quartz veins. **Basic dykes** cut across the peraluminous granite in the NW-SE direction. **Quartz veins** cut across the ophiolitic mélange. Some of them are beryl bearing veins –if present- they are usually surrounded by phlogopite schist which replaces tremolite-actinolite pockets, may be after a pyroxene protolith. **The Wadi**

deposits of W. Um Addebaa (about 3 km long), contains abundant beryl fragments as a result of ancient mines working.

GEOCHEMISTRY

The geochemical analyses of nine samples of peraluminous granites were carried out. The obtained data are listed in Table (1).

Geochemical Characteristics

The studied granite is relatively enriched in SiO_2 , Al_2O_3 , Na_2O and K_2O contents and relatively low in TiO_2 , MgO , CaO , FeO & MnO contents (Table 1). The relatively high content of alumina (av. 14.77%) reflects the high muscovite and garnet contents, whereas the low concentrations of Fe_2O_3 , MgO , CaO and TiO_2 , reveal the lack of ferro-magnesium minerals. The relatively high Na and K content reflects the abundance of feldspar minerals. It displays enrichment in incompatible elements, especially K and Rb and depletion of High Field Strength Elements (HFSE) such as Nb and Zr (Table 1). It is characterized by low contents of rare earth elements (REE = 3-29 ppm), (Table 1).

The studied peraluminous granite possesses an average 6.7 ppm of Be; so it is believed that this granite is the source of beryl mineralization in Wadi El Gemal area.

On the basis of R1-R2 discrimination diagram of De La-Roche et al. (1980), the studied peraluminous granite has syenogranite to monzogranite characters (Fig. 7). According to Peccerillo and Taylor (1976), the most samples of the studied granite belong to calc-alkaline series (Fig. 8).

Based on Maniar and Piccoli, (1989), the studied granite samples fall in the peraluminous field (Fig. 9). According to binary variation diagram of Chappell and White (1974), the studied granite samples fall within the field of I-type granite (Fig. 10). Based on R1-R2 tectonic discrimination diagram of Bachelor and Bowden (1985), the studied

Table 1: Geochemical analysis data of the peraluminous granite, Um Addebaa area, SED, Egypt

	UDG-1	UDG-2	UDG-3	UDG-4	UDG-5	UDG-6	UDG-7	UDG-8	UDG-9	Average
Major Oxides										
SiO ₂	73.15	72.8	74.59	72.75	75.42	75.27	74.35	73.78	74.45	74.06
Al ₂ O ₃	14.9	14.72	14.92	14.54	14.87	14.95	14.72	14.56	14.76	14.77
Fe ₂ O ₃ (T)	2.08	2.1	1.41	1.84	0.97	0.98	0.73	0.89	0.94	1.33
MnO	0.816	0.851	0.475	0.566	0.176	0.082	0.102	0.111	0.123	0.37
MgO	0.09	0.09	0.07	0.07	0.13	0.12	0.07	0.11	0.07	0.09
CaO	1.13	1.2	1.23	1.17	1.36	1.44	1.38	1.46	1.39	1.31
Na ₂ O	4.04	4.42	4.71	4.44	5.28	5.53	5.4	5.52	5.37	4.97
K ₂ O	2.67	2.35	2.63	2.68	1.85	1.71	1.81	1.47	1.6	2.09
TiO ₂	0.017	0.011	0.011	0.012	0.013	0.016	0.005	0.016	0.013	0.01
P ₂ O ₅	0.05	0.04	0.03	0.05	0.05	0.06	0.03	0.03	0.04	0.04
LOI	1.27	1.2	0.93	0.97	0.79	0.82	0.31	0.93	0.86	0.9
Total	100.2	99.76	101	99.08	100.9	101	98.9	98.87	99.62	99.93
Trace Elements										
Au	< 1	10	< 1	< 1	< 1	< 1	< 1	< 1	< 1	10
Ag	< 0.5	< 0.5	< 0.5	< 0.5	< 0.5	< 0.5	< 0.5	< 0.5	< 0.5	-
As	25	23	31	52	2	10	1	< 1	3	18.38
Ba	18	16	14	16	15	42	12	18	11	18
Be	6	6	6	5	7	12	6	6	6	6.67
Bi	22	15	24	28	38	30	32	35	35	28.78
Br	2.4	< 0.5	< 0.5	< 0.5	< 0.5	< 0.5	< 0.5	< 0.5	< 0.5	2.4
Cd	1.1	1.1	1	1.2	< 0.5	< 0.5	< 0.5	< 0.5	< 0.5	1.1
Co	< 0.1	2.6	< 0.1	< 0.1	3.2	< 0.1	< 0.1	< 0.1	< 0.1	2.9
Cr	37.3	51.9	< 0.5	42.9	< 0.5	18.1	< 0.5	17.4	16.5	30.68
Cs	9.5	6.1	8.6	8.2	5.9	7.8	6.6	3.3	6.3	6.92
Cu	15	12	13	21	< 1	4	8	3	< 1	10.86
Hf	11.8	11.1	8.7	9.6	12.2	9.7	8.6	8.3	9.3	9.92
Hg	< 1	< 1	< 1	< 1	< 1	< 1	< 1	< 1	< 1	-
Ir	< 1	< 1	< 1	< 1	< 1	< 1	< 1	< 1	< 1	-
Mo	< 2	< 2	< 2	< 2	< 2	< 2	< 2	< 2	< 2	-
Ni	3	3	2	3	3	2	4	3	1	2.67
Pb	130	102	135	159	47	64	54	49	48	87.56
Rb	390	300	330	310	220	220	230	220	160	264.44
Sn	11	13	8	10	7	6	5	6	5	7.89
Sb	0.3	0.4	0.7	0.7	< 0.1	1	< 0.1	0.2	< 0.1	0.55
S	0.156	0.083	0.106	0.129	0.016	0.031	0.019	0.016	0.011	0.06
Sc	9.05	8.66	6.33	7.01	5	2.97	3.23	2.95	3.61	5.42
Se	< 0.5	< 0.5	13.8	12.4	6.1	6.4	< 0.5	< 0.5	< 0.5	9.68
Sr	27	27	28	28	24	37	22	26	21	26.67
Nb	21	19	15	18	16	28	14	14	13	17.56
Ta	< 0.3	< 0.3	2.8	< 0.3	< 0.3	10.3	< 0.3	< 0.3	< 0.3	6.55
Th	4.7	2.9	4	3.5	5.2	5.7	4.4	4.2	5.4	4.44
U	20.4	17	16.3	15.8	25.6	23.2	16.8	17.4	18.2	18.97
V	13	7	6	8	14	7	6	7	6	8.22
W	< 1	< 1	< 1	< 1	< 1	< 1	< 1	< 1	< 1	-
Ga	34	33	28	31	28	26	26	26	27	28.78
Y	392	415	255	295	155	77	97	102	112	211.11
Zn	338	282	322	418	49	102	58	47	47	184.78
Zr	171	137	124	131	200	140	115	120	128	140.67
REEs										
La	8.24	5.79	6.16	6.75	8.08	8.31	6.41	5.95	6.86	6.95
Ce	46	34	35	31	26	23	21	20	24	28.89
Nd	12	10	16	18	20	20	12	10	12	14.44
Sm	9.03	7.34	6.9	7.33	7.89	6.56	6.32	5.88	6.84	7.12
Eu	< 0.2	< 0.2	< 0.2	< 0.2	< 0.2	< 0.2	< 0.2	< 0.2	< 0.2	-
Tb	8.2	10.3	6.3	6.8	4	2.9	2.9	2.7	3.3	5.27
Yb	24.6	24.1	17.2	19.5	11.8	5.26	7.28	7.36	8.16	13.92
Lu	4.51	4.26	3.36	3.65	2.76	1.54	1.71	1.8	2.09	2.85

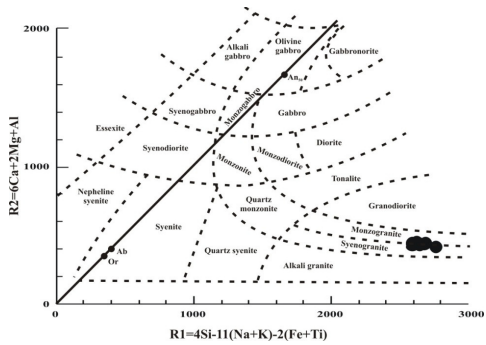


Fig. 7: R_1 - R_2 diagram for the studied granodiorite and monzogranite according to De La Roche et al. (1980)

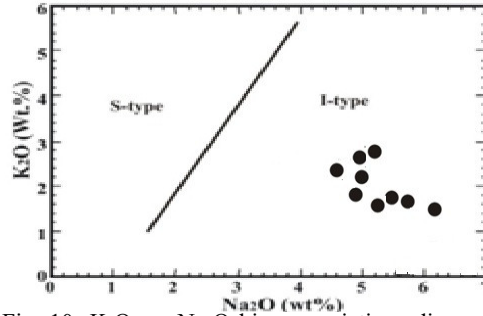


Fig. 10: K_2O vs. Na_2O binary variation diagram (according to Chappel and White, 1974) of the studied peraluminous granites, Um Addebaa area, SED, Egypt

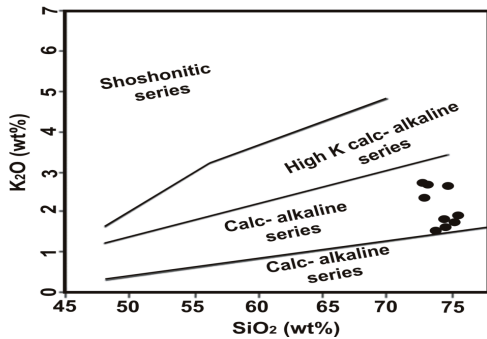


Fig. 8: SiO_2 versus K_2O diagram according to Peccerillo and Taylor (1976) for the studied peraluminous granite, Um Addebaa area, SED, Egypt

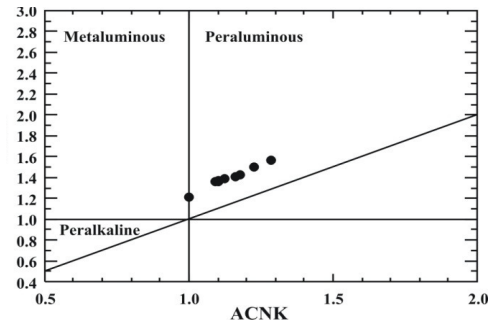


Fig. 9: A/NK vs. A/CNK binary diagram for the studied peraluminous granites, according to Maniar and Piccoli, (1989), Um Addebaa area, SED, Egypt

granite belongs to Syn-collision setting field (Fig. 11). According to Ab-Qz-Or diagram of Tuttle and Bowen (1958) and after Luth et al., (1964) the studied granite emplaced at relatively shallower depth (water pressure 3 - 2 kb; Fig. 12) in the crust and crystallized at temperature range from 800 to 760 $^{\circ}C$ (Fig. 13).

Based on the spiderdiagram of normalized trace elements relative to the chondrites of Thompson (1982), the studied granite shows a marked enrichment of Rb, Th, K, La, Ce, Nd, Tb, Yb, Sm, Hf and Y and a marked deple-

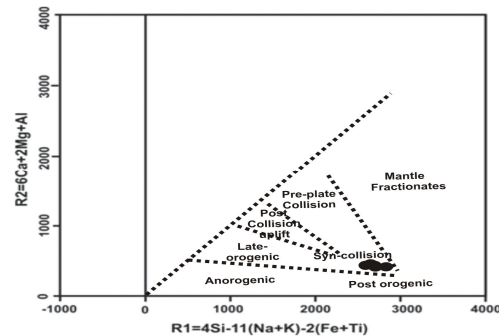


Fig. 11: R_1 - R_2 diagram according to Bachelor & Bowden (1985) of tectonic settings of the studied peraluminous granite, Um Addebaa area, SED, Egypt

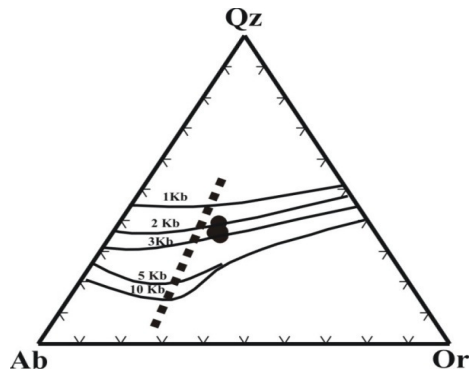


Fig. 12: Ab-Qz-Or diagram for the studied granite. The dashed lines represent the minimum melting points in the granite system at different water-vapor pressure. 1, 2 & 3 kb according to Tuttle and Bowen (1958), 5 & 10 kb according to Luth et al. (1964), Um Addebaa area, SED, Egypt

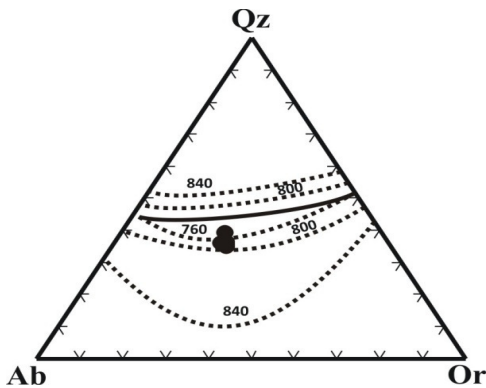


Fig. 13: Ab-Qz-Or diagram for the studied granite, according to Luth et al., (1964), Um Addebaa area, SED, Egypt

tion of Ti, whereas Sr and Ba values around the unity (Fig. 14).

According to spider diagram plot of Taylor & McLennan (1985) the studied granite-sare characterized by high content of Cs, Rb, U, Tb, Y, Yb and moderate enrichment of Ta, Hf, Sm & K. Otherwise, it has very depletion in Ba, Ti & Sr while it has moderate depletion of La, Ce & Nd (Fig. 15). The strong enrichment content of some elements is due to

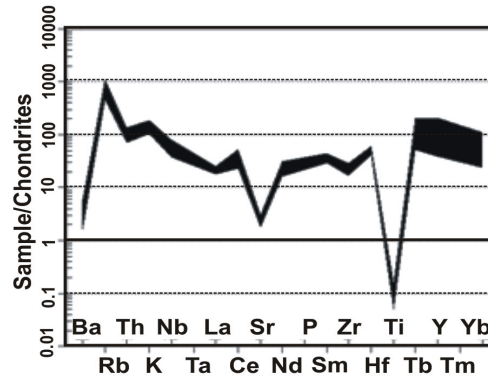


Fig. 14: Spider diagram of normalized trace elements for studied peraluminous granite, Um Addebaa area, SED, Egypt. Samples are normalized to chondrites of Thompson (1982)

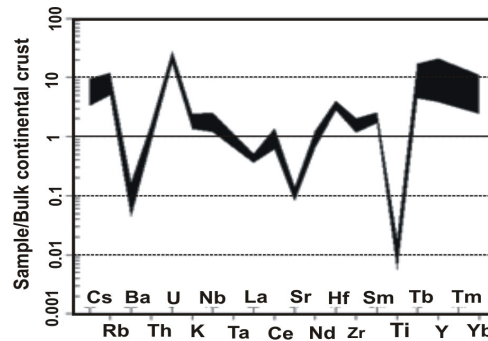


Fig. 15: Spider diagram of normalized REE for studied peraluminous granite, Um Addebaa area, SED, Egypt. Samples are normalized to Bulk continental crust of Taylor and McLennan, (1995)

the presence of some accessory minerals as xenotime and zircon.

RADIOMETRY

Spectrometric Study

Gamma-ray spectrometry has been carried out on the studied peraluminous granite, using GS-512 spectrometer. The measurements are expressed in ppm for eU

& eTh and in percent for K (Table 2). The radioelements of the peraluminous granites possess high average values of the K%, eU, eTh contents and their ratios. The average values of eU content are higher than the average values of eTh content. The relation of the radioelement concentrations in the studied peraluminous granite to those of the crustal igneous rocks after IAEA (1979), Boyle (1982), Adams et al. (1959) and Clarke et al. (1966) are listed in Table (2) and shows the following features:- The average values of K, eTh contents are the lesser than those the corresponding values in the crustal average, while the average values of eU content are higher than those the corresponding values in the crustal average. The average values of the eU content of the peraluminous granites are higher than the twice Clarke (Clarke value for eU =4 ppm and eTh =18-20 ppm), but the average values of the eTh content are lesser than the twice Clarke values. From the above correlation (Table 3), we can conclude that the peraluminous granites at Um Addebaa area are relatively abnormal case as the corresponding values in the crustal average and there are some high values of radioactive elements. The termuraniferous should be applied to this granite, which contains eU (12 ppm) higher than twice of Clarke value. The term fertile should be applied according to Gangloff (1970), where the uranium content varies between 4-22 ppm.

The correlation diagrams of eU vs. eTh, eU vs. eU/eTh and eTh vs. eU/eTh are shown on Figs. (16 -18). From these diagrams, the following could be summarized:-

Plot of eU vs. eTh correlation diagram showed that there is strongly positive correlation ($r = 0.63$) between eU and eTh in the peraluminous granite. Plot of eU vs. eU/eTh correlation diagram showed that there is moderately positive correlation ($r = 0.44$) between eU and eU/eTh ratio in the peralumi-

Table 2: Statistics of spectrometric data and their ratios of the peraluminous granite at Um Addebaa area, Um Addebaa area, SED, Egypt

Peraluminous granite (N=20)						
	K%	eU (ppm)	eTh (ppm)	eU/eTh	eTh/eU	eTh/K
Minimum (Min.)	1	4	3	0.80	0.24	1.14
Maximum (Max.)	5.5	22	15	4.30	1.33	3
Range	1-5.5	4-22	3-15	0.80-4.30	0.24-1.33	1.14-3
Mean (X)	3.93	12.77	7.77	1.80	0.67	1.95
Crustal acidic igneous rocks (after IAEA, 1979 and Boyle, 1982)						
Average	4	4.5	18	0.25	-	-
Range	-	1-12	5-20	0.1-0.5	-	-
Adams et al, 1959 Clarke et.al, 1966						
Average	-	4	19	0.25	-	-
Range	-	1-9	18-20	-	-	-

N = number of measurements

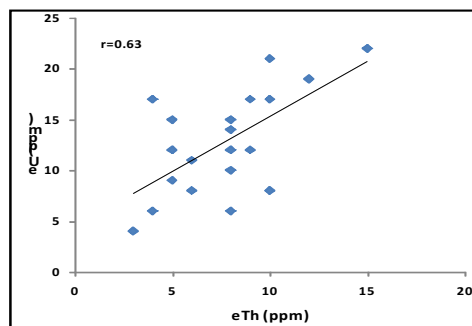


Fig. 16: Correlation diagram of eTh vs. eU of the peraluminous granite, Um Addebaa area, SED, Egypt

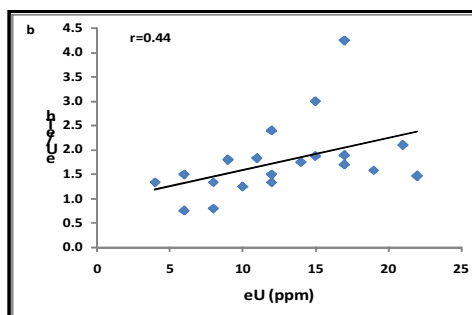


Fig. 17: Correlation diagram of eU vs. eU/eTh of the peraluminous granite, Um Addebaa area, SED, Egypt

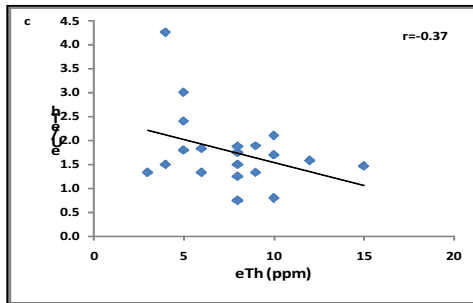


Fig. 18: Correlation diagram of eTh vs. eU/eTh of the peraluminous granite, Um Addebaa area, SED, Egypt

nous granite. Plot of eTh vs. eU/eTh correlation diagram showed that there is moderate negative correlation ($r = -0.37$) between eTh and eU/eTh ratio in the peraluminous granite (Khaleal and Mahmoud, 2009).

Geochemical Distribution of Uranium and Thorium

From Table (1), the peraluminous granite samples show U content ranging from 15.8 – 25.6 with an average of 18.9, while Th content ranging from 2.9 to 5.7 with an average of 4.4. Also, this agrees with the spectrometric values that U content is more than Th content. The high U/Th ratio of the peraluminous granite may be due to their enrichment in radioactive accessory minerals such as zircon, xenotime and allanite.

MINERALOGY

Microscopic investigations, scanning electron microscopy (SEM), and electron probe micro-analyses (EPMA) were used to identify and study minerals present in the peraluminous granite.

Generally, some minerals such as beryl and tourmaline are observed by naked eye in the ophiolitic mélange surrounding the peraluminous granite. In the peraluminous granite itself, garnet (spessartine) is observed also by naked eye. Other some minerals such as zir-

con and xenotime are detected by SEM.

Spessartine $Mn_3^{+2}Al_2(SiO_4)_3$ is reddish orange in color (Fig. 19). It was confirmed by XRD techniques (Fig. 20). SEM technique is used for analyzing the garnet crystals from core to rim {Figs. 21 (a–d) and Table 3} as indicating by Zoning in spessartine crystals. The composition differs from core to the rim due to the variation in the ratio of Fe and CaO. As Mn increases in the core more than the rim whereas Fe indicates vice versa, i. e. it increases in the rim and decrease in the core. Zircon (Figs. 22.a&b) and xenotime (Fig. 23) are also recorded in the peraluminous granites. Tables (4&5) show scan analysis values for muscovite and uranium oxide detected in the studied peraluminous granite, respectively.

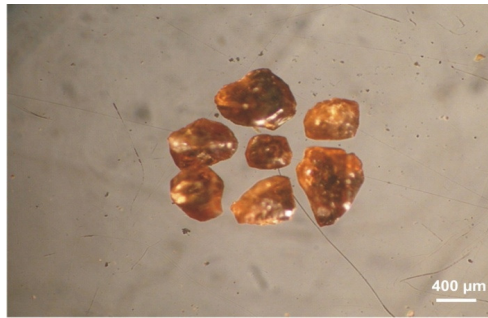


Fig. 19: Reddish orange colored spessartine garnet in peraluminous granites at Um Addebaa area, SED, Egypt

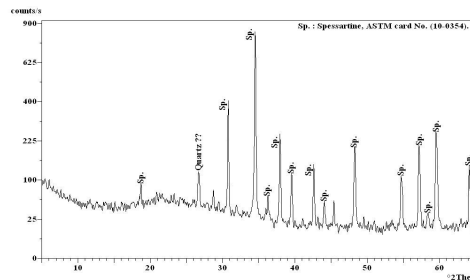


Fig. 20: XRD pattern for garnet (spessartine) in peraluminous granites in Um Addebaa area, SED, Egypt

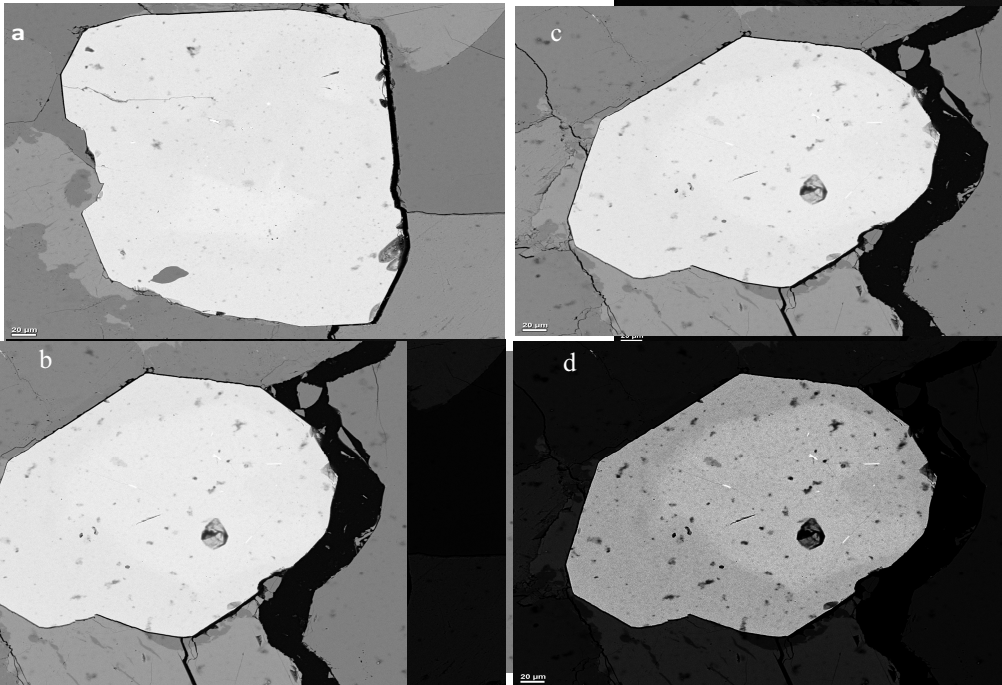


Fig. 21 (a-d): SEM photos of spessartine in peraluminous granites in Um Addebaa area, SED, Egypt. Note zoning from core to rim on Figs (b & d)

Table 3: Scan analysis values of spessartine (core and rim) in the studied peraluminous granites

Sample	MgO	Al ₂ O ₃	SiO ₂	Y ₂ O ₃	CaO	TiO ₂	MnO	FeO	Total
UDG1-Core	0.32	20.6	36.07	0.43	4.9	0.14	15.89	21.7	100.05
UDG1-Rim	0.45	20.52	35.78	0.35	1.76	0.15	13.75	26.8	99.56
UDG2-Core	0.45	20.46	35.51	1.75	2.94	0.17	11.71	26.12	99.12
UDG2-Rim	0.35	20.48	36.34	0.37	2.36	0.21	12.73	27.03	99.85
UDG3-Core	0.36	20.37	35.24	1.97	3.59	0.12	12.61	23.57	97.83
UDG3-Rim	0.28	20.56	35.97	0.33	1.54	0.24	13.45	27.05	99.43
UDG4-Core	0.44	20.67	35.75	1.64	3.42	0.13	18.78	18.8	99.63
UDG4-Rim	0.43	20.75	35.99	0.8	2.14	0.28	17.44	22.6	100.43
UDG5-Core	0.28	20.46	35.71	1.38	3.54	0.29	18.22	18.84	98.72
UDG5-Rim	0.36	20.82	36.29	0.28	1.73	0.14	16.93	23.86	100.4
UDG6-Core	0.73	20.82	35.16	2.27	3.49	0.26	7.8	29.46	100
UDG6-Rim	0.4	20.68	36.31	0.49	2.31	0.18	7.89	30.96	99.21
UDG9-Core	0.33	20.62	36.22	0.48	3.27	0.12	6.33	31.93	99.21
UDG9-Rim	0.35	20.24	35.53	0.54	1.46	0.2	8.6	30.71	97.64

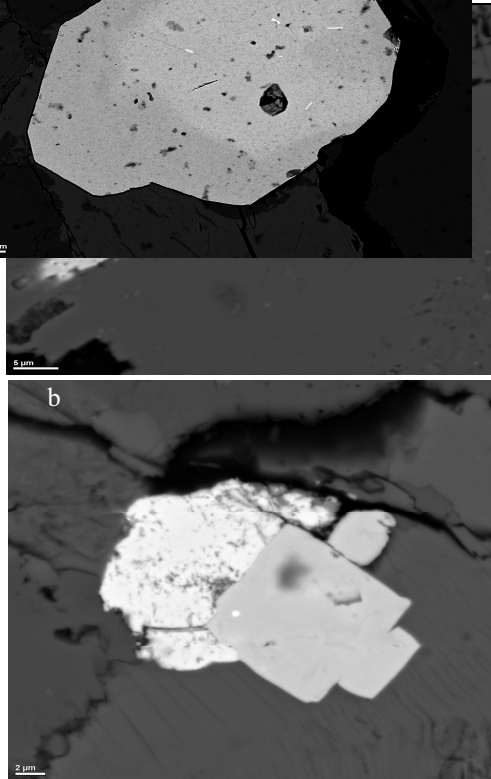


Fig. 22 (a & b): SEM photos of zircon in peraluminous granite at W. Um Addebaa area, SED, Egypt

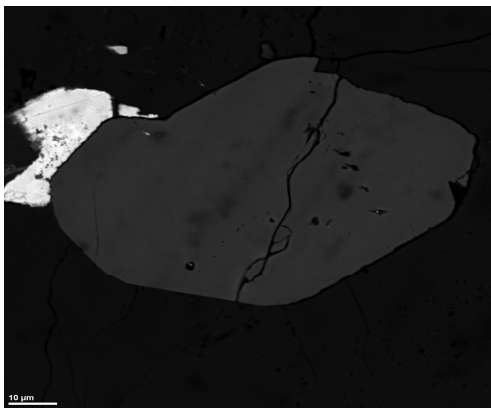


Fig. 23: SEM photo of xenotime in peraluminous granite at W. Um Addebaa area, SED, Egypt

Table 4: Scan analysis values of muscovite in the studied peraluminous granites

Sample	Na ₂ O	MgO	Al ₂ O ₃	SiO ₂	K ₂ O	MnO	FeO	Total
UDG9 Musc.	0.29	0.62	33.29	46.97	10	0.43	3	94.6

Table 5: Scan analysis values of uranophane in the studied peraluminous granites

Sample	SiO ₂	Y ₂ O ₃	ZrO ₂	pbO	UO ₂	Total
UDG2 Uranium Oxide	3.71	7.18	3.91	6.88	76.42	98.1

MICROPROBE STUDY

Mineral composition for many grains of garnet are determined on the JEOL JXA-733 Superprobe; operating conditions (Table, 6) at the Microscopy and Microanalyses Facility, University of New Brunswick (UNB), Fredericton, New Brunswick, Canada. The aim of the microprobe analysis is to contrast the garnet chemistry and/or composition for different parts of the peraluminous granites and also to get a better understanding of its final concentrate composition.

Three grains of garnet are chemically analyzed by microprobe along profiles {Fig. 24 (A-C)}. For each grain, eight element oxides are analyzed at the laboratories of UNB, Canada. The data is listed in Table (7). Generally, garnet is mainly spessartine with a core rich in CaO, MgO, TiO₂ and Y₂O₃, while the rim is enriched in FeO and Al₂O₃ and SiO₂. MnO shows variable enrichment.

Some bar diagrams were constructed to illustrate some ratios of oxides in the studied spessartine grains (Figs 25-27).

Table 6: Microprobe analysis conditions

Name	Z	Line	Standard	Xtal	Spec	Pos	SHigh	Slow	UHigh	ULow	Bias	Gain	Base	Window	KV	Sinten
Mg	12	K	GRTGM	TAP	1	107,794	4	4.5	4	4.5	1740	10	18	55	15	49.8577
Al	13	K	GRTGM	TAP	1	90,979	3	5	3	5	1720	10	18	55	15	157.7501
Si	14	K	GRTGM	TAP	1	77,816	4	5.5	4.5	5.5	1710	10	17	55	15	259.7478
Ca4	20	K	Cpic511	PET	4	107,559	4	4	4	4	1800	12	16	40	15	104.0805
Ti	22	K	ilm	PET	4	87,941	4	4	4	4	1800	12	18	50	15	225.0537
Mn	25	K	Bust	LIF	3	145,701	4	4	4	4	1780	8	17	35	15	20.2888
Fe	26	K	HMT	LIF	3	134,171	4	4	4	4	1790	8	20	45	15	95.995
Y2	39	L	Yag	TAP	2	68,078	1.5	1.8	1.5	1.8	1720	8	15	40	15	249.1647

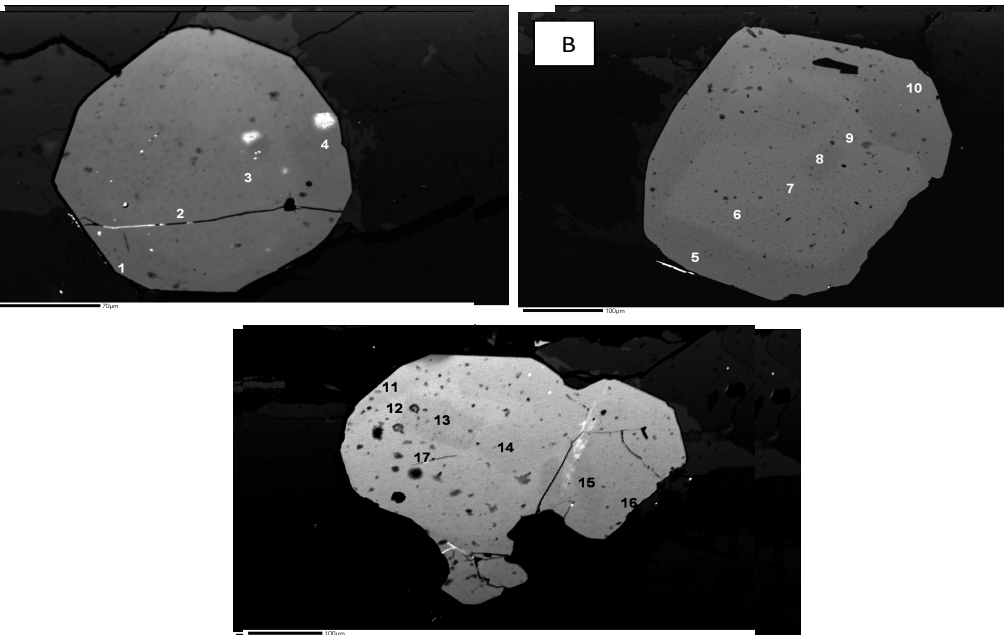


Fig. 24 (A to C): Back-scattered- electron image showing profiles of spots of microprobe analyses in three (3) garnet grains respectively in the peraluminous granites, Um Addebaa area, SED, Egypt

Table 7: Microprobe analysis of three spessartine grains Um Addebaa area, SED, Egypt

Pt	MgO	Al ₂ O ₃	SiO ₂	CaO	TiO ₂	MnO	FeO	Y ₂ O ₃	Total
1	0.134	20.11	35.23	2.8135	0.0009	13.96	25.65	0.1284	98.02
2	0.1791	19.99	34.69	3.54	0.0273	13.21	24.53	1.2727	97.44
3	0.1706	20.1	34.36	3.31	0.0303	13.47	24.98	1.2828	97.7
4	0.1399	20.22	35.43	2.8239	0	14.08	25.96	0.1328	98.79
5	0.1297	20.32	35.5	2.7558	0	13.64	26.73	0.1813	99.26
6	0.1366	20.23	35.08	3.35	0.0197	14.96	23.39	1.5497	98.71
7	0.1283	20.24	35.02	3.45	0.222	15.09	23.22	1.6573	98.82
8	0.1121	20.13	35.67	4.17	0.0164	14.81	23.8	0.6793	99.38
9	0.1436	20.17	35.29	3.89	0.012	13.97	23.35	1.686	98.51
10	0.1249	20.42	36.2	3.13	0.0049	13.33	26.47	0.1831	99.86
11	0.1293	20.47	36.13	2.5939	0.0105	14.38	25.35	0.2406	99.3
12	0.1591	20.31	35.41	3.32	0.0107	13.75	23.76	1.5735	98.31
13	0.1275	20.17	35.84	3.88	0.0217	14.71	23.54	0.639	98.92
14	0.1302	20.24	35.76	4.26	0.0152	14.8	22.74	0.7075	98.65
15	0.1094	20.61	36.35	4.38	0.0107	13.94	24.38	0	99.78
16	0.1308	20.52	36.11	1.9463	0	14.44	26.18	0.0619	99.39
17	0.1619	20.3	35.29	3.4	0.0296	13.99	23.43	1.8443	98.46

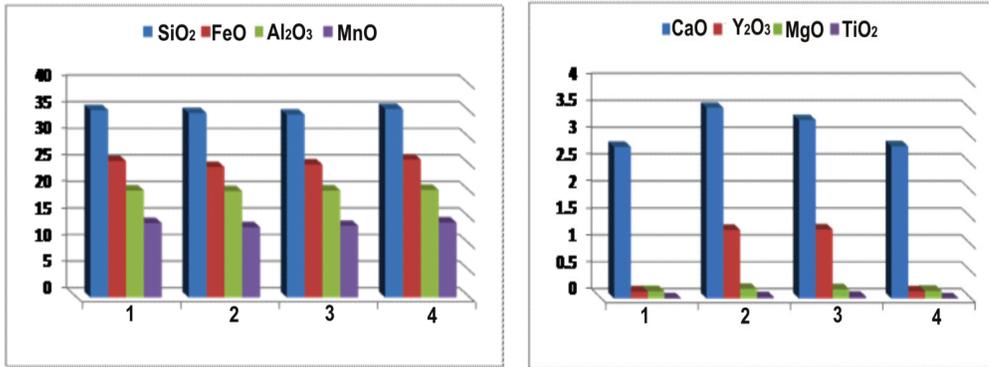


Fig. 25: Bar-diagram of some oxides in spessartine grain no. A

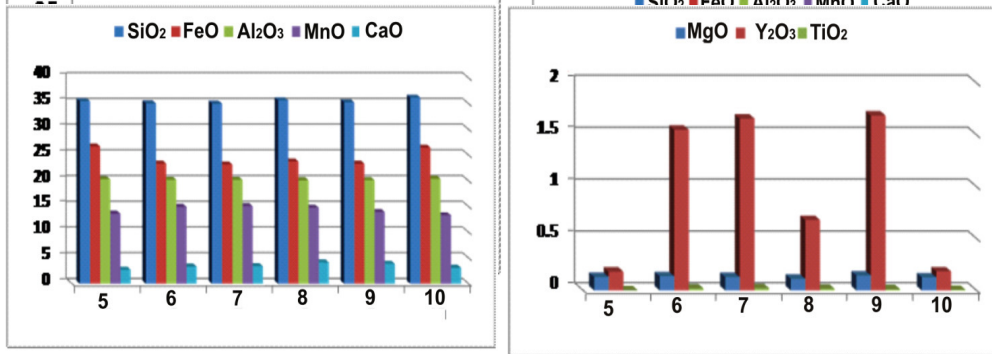


Fig. 26: Bar-diagram of some oxides in spessartine grain no. B

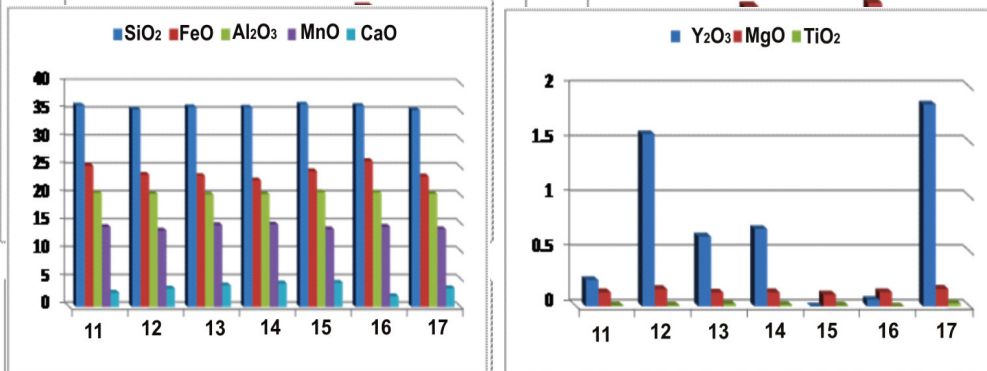


Fig. 27: Bar-diagram of some oxides in spessartine grain no. B

CONCLUSIONS

The rocks exposed in Wadi Um Addebaa area include: ophiolitic metagabbro, ophiolitic mélange, peraluminous granite and post granite dykes and veins. The most common feature in the peraluminous granite is the presence of spessartine garnet aligned in monomineralic bands (1m thick) in parts along the periphery with surrounding schists. The Wadi deposits of W. Um Addebaa (about 2 km long) contains abundant beryl fractions.

The peraluminous granite is mainly composed of K-feldspar, sodic plagioclase (An 5-15), quartz, muscovite and biotite. Sericite and chlorite are secondary minerals. Spessartine, tourmaline, zircon, allanite and opaques are accessory minerals. Myrmekitic texture is common indicating metasomatic process.

The presence of muscovite flakes reflects the peraluminous nature of these granites. The presence of two feldspars suggests that the muscovite granites are mostly subsolvus and crystallized under high water pressure.

The deformational features of the studied granite are expressed by bent plagioclase lamellae, distorted microcline twinning, deformed mica flakes, strongly undulatory quartz, development of myrmekite and recrystallization of feldspars into fine-grained aggregates. All these features point to subsolidus. Such deformation should be the result of extensive regional thrusting to which the area had been subjected.

The studied peraluminous granite crystallized from relatively soda rich magma, has peraluminous character, I-type, calc-alkaline affinity and emplaced in syn-collision setting. at relatively shallower depth (water pressure 3-2 kb) in the crust and crystallized at temperature range from 800 to 760 C°.

It possesses high content of LILE (Rb, Y & Zr) and has a moderate to high content of HFSE (Cu, Zn, Pb, As, Bi & W).

It possesses an average 6.7 ppm of Be;

hence, it is believed that this granite is the source of beryl mineralization in Wadi El Gemal area.

The studied granite has relatively high alkali content ($K_2O + Na_2O$) and high Al_2O_3 contents and relatively low TiO_2 , MgO, CaO, FeO & MnO contents.

Comparing the studied granite relative to the chondrites, it shows a marked enrichment of Rb, Th, K, La, Ce, Nd, Tb, Yb, Sm, Hf and Y and depleted in Ti, whereas Sr and Ba values around the unity. The studied granites are characterized by high content of Cs, Rb, U, Tb, Y, Yb and moderate enrichment of Ta, Hf, Sm & K comparing it relative to Bulk continental crust. Otherwise, it has very depletion in Ba, Ti & Sr while it has moderate depletion of La, Ce & Nd. The strong enrichment content of some elements is due to the presence of some accessory minerals like xenotime, allanite and zircon.

Radiometrically, the studied peraluminous granite shows chemically uranium contents with an average of 19 ppm and thorium contents with an average of 4.5 ppm. This also agrees with the spectrometric values that U content is more than Th content. Uranium content is more than twice Clark value (4 ppm), while eTh content is too less than Clark value (18-20 ppm) suggesting that it is fertile granite. The high U/Th ratio of the studied peraluminous granite may be due to their enrichment in radioactive accessory minerals such as zircon.

Some minerals such as beryl and tourmaline are observed by naked eye in the schists of the ophiolitic mélange surrounding the peraluminous granite. In the peraluminous granite itself garnet (spessartine) is observed also by naked eye. Other some minerals such as zircon and xenotime are detected by SEM.

From microprobe study, garnet is mainly spessartine with a core rich in CaO, MgO and Y_2O_3 , while the rim is enriched in FeO and Al_2O_3 and SiO_2 . MnO shows variable en-

richment.

Acknowledgements

The author wishes to express his deep gratitude to Prof. David Lentz (Prof. of economic geology) University of New Brunswick (UNB) for his encouragement and kind help, to Dr. Douglas C. Hall (Microscopy and Microanalysis Facility, University of New Brunswick (UNB), Canada) for kind help during the laboratory work at the laboratories of UNB and to members of Abu Rusheid-Halayeb Project NMA Egypt.

REFERENCES

- Adams, J.A.S., Osmond, Y.K., and Rogers, J.J.W., 1959. The geochemistry of thorium and uranium, *Physics and Chemistry of the Earth*. Program Press, London, 3, 298-348.
- Ashworth, J. R., 1979. Genesis of the Skagit Gneiss migmatites, Washington, and the distinction between possible mechanisms of migmatization: Discussion and reply. *Geological Society of America Bulletin*, 90, 887-888.
- Batchelor, R.A., and Bowden, P., 1985. Petrogenetic interpretation of granitoid rock series using multi – cationic parameters. *Chem. Geol.*, 48, 43-55.
- Barbey, P., Ma Caudiere, J. and Nzenti, J.P., 1990. High-pressure dehydration melting of metapelites: evidence from the migmatites of Yaound (Cameroon). *J. Petro.*, 31, 401- 427.
- Boyle, R. W., 1982. Geochemical prospecting for thorium and uranium deposits. *Develop. Economic, Geol.*, 16, El Sevier, Amsterdam, p.489.
- Chappell, B.W. and White, A. J. R., 1974. Two contrasting granite types: *Pacific Geol.*, 8, 173-174.
- Clarke, S. P., Peterman, Z. E., and Heier, K. S., 1966. Abundance of uranium, thorium and potassium, In: S.P. Clarke 4,J (Editor), *Handbook of physical contacts*, *Geol. Soc. Am. Mem.* 97 sections 24, 521-541.
- Clemens, J.D. and Wall, V.J., 1981. Crystallisation and origin of some paraluminous (S-type) granitic magmas. *Canad. Mineral.*, 19, 111-132.
- Debon, F., Le Fort P., Sheppard, S. M. F. and Sonet, J., 1986. The four plutonic belts of the Transhimalaya-Himalaya: a chemical mineralogical isotopic and chronological synthesis along a Tibet-Nepal section. *J. Petrol.*, 27, 219-250.
- Deer, W. A., Howie, R. A. and Zussman, J., 1992. An introduction to the rock forming minerals. Longman group limited, England. Second edition.
- De La Roche, H.; Leterrier, J.; Grandclaude, P. and Marchal, M., 1980. A classification of volcanic and plutonic rocks using R1 – R2 diagram and major element analyses; Its relationships with current nomenclature. *Chem. Geol.*, 29, 183 – 210.
- Fyfe, W.S., 1969. Some thoughts on granitic magmas, In: G. Newall and N. Rast (eds.), *Mechanism of Igneous Intrusions*. *Geol. J. Spec.* 2, 201- 216.
- Gangloff, A., 1970. Notes somaries la geologie des principaux districts uraniferes studies par la CEA, In: *Uranium exploration geology*, I.A.E.A., Vienna, 77-105 (IAEA-391-16).
- Greenberg, J. K., 1981. Characteristics and origin of Egyptian younger granites. *Geol. Soc. America Bull.*, part I, 92, 224-256.
- Greiling, R. O., Kroner, A, El Ramly, M. F. and Rashwan, A. A., 1987. Structural relationships between the southern and central parts of the Eastern Desert of Egypt; Details of a fold and thrust belt. In: El Gaby, Greiling, R. (eds.). *The Pan-African belt of NE Africa and adjacent areas- tectonic evolution and economic aspects of a late Proterozoic orogen*. Vieweg. Wiesbaden. 121-145.
- Gronet, L.P. and Silver, L.T., 1983. Rare earth element distributions among minerals in a granodiorite and their petrogenetic implications.

- Geochim. Cosmochim Acta, 47, 925-939.
- Hassan, M., El-Bakry ,H., Al-Amin, and Al Bassiony, Q., 1984. Geochemical orientation survey of tungsten mineralization in arid conditions, eastern desert, Egypt Bul. Fac Sci Zagazig Univ . 6, 38-54 .
- Hume, W. F., 1934. Geology of Egypt. V. II, Part I. The metamorphic Rocks. Geol. Surv. Egypt. Government Press, Cairo, 300 P.
- International Atomic Energy Agency (IAEA), 1979. Gamma ray surveys in uranium exploration, Technical Report Series, paper no.186, 90p.Vienna.
- Ibrahim, M.E., Saleh, G.M. and Abd EL-Naby, H. H., 2001. Uranium mineralization in the two mica granite of Gabal Ribdab area, South Eastern Desert, Egypt. Applied Radiation and Isotopes, 55, 861-872.
- Inger, S. and Harris, N., 1993. Geochemical constraints on leucogranite magmatism in the Langtang Valley.Nepal Himalaya.J.Petrol 34, 345-368.
- Khaleal, F. M., and Mahmoud, M. A., 2009. Radiometric and mineralogical studies on the muscovite granites at Wadi El Gemal area, South-eastern Desert, Egypt.Sci. J. Fac. Sci. Minufia Univ. XXIII(2), 121-147.
- Luth, W. C., Jams, R. H. and Tuttle, O. F., 1964. The granite system at pressure of 4 to 10 kilobars. J. Geophys. Res., 69, 759-773.
- Mahmoud, M., 2009. Highlight on the geology, geochemistry and spectrometry of the muscovite granites at Wadi El Gemal area, South Eastern Desert, Egypt, Ph.D. Thesis, Suez Canal University, Egypt, 227p.
- Mahood, G. A., Nibler, G. E. and Halliday, A. N., 1996. Zoning patterns and petrologic processes in peraluminous magma chambers: Hall Canyon pluton, Panamint Mountains, California: Geological Society of America Bulletin, 108, 437-453.
- Maniar, P.D., and Piccoli, P.M., 1989. Tectonic discrimination of granitoids. Geol. Soc. Am. Bull., 101, 635-643.
- Middlemost, E.A.K., 1985. Magmas and magmatic rocks. An introduction to igneous petrology. Longmen Group Ltd, Essex, 266p.
- Mohamed F. H. and Hassanen M. A., 1997. Geochemistry and petrogenesis of Sikait leucogranite, Egypt: an example of S-type granite in a metapelitic sequence. Geol. Rundsch. 86, 81-92.
- Nabelek, P. I., Lin, M. and Sirbescu, M., 2001. Thermo-rheological, shear-heating model for leucogranite generation, metamorphism and deformation during the Proterozoic Trans-Hudson orogeny, Black Hills, South Dakota. Tectonophysics, 342, 371-388.
- Omar, S. A., 2001. Characterization and evaluation of some beryl occurrences in the Eastern Desert, Egypt. Ph. D. Thesis, Cairo univ. Egypt, 258 p.
- Paterson, S.R., Vernon, R. H., Tobisch, O.H., 1989. Preview of criteria for the identification of magmatic and tectonic foliations in granitoids. J. structural Geol. 11, 340-363.
- Pearce, J. A., Harris, N.B.W. and Tindle, A.G., 1984. Trace element discrimination diagrams for the tectonic interpretation of granitic rocks. J. Petrol. 25, 956-983.
- Peccerillo, A. and Taylor, S. R., 1976. Geochemistry of Eocene calc-alkaline rocks from the Kastamonu area, northern Turkey. Contr. Min. Petrol., 58, 63-81
- Philips, G. N.,Wall,V.J. and Clemens, J.D., 1981. Petrology of the Sorathbogic batholith: A cordierite-bearing granite. Can. Mineral 19, 47-63.
- Royden, L. H., 1993. The steady-state thermal structure of eroding orogenic belts and accretionary prisms; J. Geophys. Res., 98. 4, 487-4,507.
- Saleh, G. M., 1997. The potentiality of uranium occurrences in Wadi Nugrus area, south Eastern Desert, Egypt. Ph. D. Thesis Mans. Univ. 171 p.

- Saleh, G. M., Abd El Naby, H. H., and Ibrahim, M. E., 2002. Granite magmatism in the Gabal Harhagit area, South Eastern Desert, Egypt: Characteristics and petrogenesis. *Egyptian J. of Geology*, 46/1, 117-126.
- Smith, P. J., 1974. Ophiolites and oceanic lithosphere nature. *London* 250, 99-100.
- Takla, M. A., and Nowier, A. M., 1980. Mineralogy and mineral chemistry of the ultramafic mass of El- Rubshi, E. D., Egypt. *Neves Jahrb. Min. Abh.*, 140/1, 17-28.
- Taylor, S. R. & McLennan, S. M., 1985. *The Continental Crust: Its Composition and Evolution*. Blackwell Scientific Publications, Oxford.
- Thompson, A. B., 1982. British Tertiary volcanic province. *Scott. J. Geol.*, 18, 49-107.
- Thompson, A. B. and Connolly, J. A. D., 1995. Melting of the continental crust: Some thermal and geological constraints on anatexis in continental collision zones and other tectonic settings. *Journal of Geophysical Research* 100, 15, 565-79.
- Tuttle, O. F. & Bowen, N. L., 1958. Origin of granite in the light of experimental studies in the system NaAlSi₃O₈-KAlSi₃O₈-SiO₃-H₂O, *Geological Society America Memoir*, 74, 1- 153.

جيولوجية وجيوكيميائية صخور الجرانيت الفوق ألمنيومي في منطقة وادي أم الضباع ، جنوب الصحراء الشرقية ، مصر

فراج محمد خليل

تقع منطقة وادي أم الضباع علي بعد حوالي ٧٠ كم جنوب غرب مدينة مرسى علم. الصخور المنكشفة في هذه المنطقة تشمل: الميتاجابرو الأفيوليتي و الميلانج الأفيوليتي و الجرانيت الفوق ألومنيومي والقواطع و العروق مابعد الجرانيت. الهدف من هذه الدراسة هو دراسة الخصائص الجيولوجية والجيوكيميائية للجرانيت الفوق ألمنيومي في منطقة وادي أم الضباع، جنوب الصحراء الشرقية، مصر. الظاهرة الأكثر شيوعا في صخر الجرانيت الفوق ألمنيومي هي وجود السبستين جارنت متراص في شرائط منتظمة في الجزء الخارجي منه (سمك ١م) عبر خط التماس مع الشبست. رواسب الوديان في وادي الضباع (حوالي ٢ كم طول) تحتوي وفرة من كسرات البريل.

أظهرت الدراسة البتروجرافية أن صخر الجرانيت الفوق ألمنيومي يتكون أساسا من البلاجيوكليز الصودي (أنورثيت ٥-١٥)، والفلسبار البوتاسي، والكوارتز، والمسكوفيت، والبيوتيت. السربست والكوريت معادن ثانوية. السبستين والألانيتوالتورمالين والزركون والمعادن القاتمة موجودة كمعادن إضافية. نسيج الميرميكيت شائع دليل علي عمليات الميتاسوماتيزم.

الخصائص الجيوكيميائية لصخر الجرانيت الفوق ألمنيومي تدل علي أن هذا الجرانيت قد تبلور من ماجما غنية بالصودا نسبيا، وهو عالي الألومنيومية، وذو أصل ناري، و كلس قلووية، و تداخل في القشرة الأرضية مزامنا للتصادم Syn-collision، علي عمق ضحل نسبيا وتحت ضغط ٢-٣ كيلوبار وتبلور عند درجة حرارة من ٨٠٠ إلي ٧٠٠ درجة. يحتوي صخر الجرانيت الفوق ألمنيومي علي محتوى عالي من عناصر الربيديوم و الاثريوم و الزركونيوم و محتوى متوسط إلي عالي من النحاس و الخارصين و الرصاص و الزرنيخ و البزموت و الولفرام. إنه يحتوي علي بريليوم بنسبة ٦,٧ جزء في المليون في المتوسط ولذلك يعتقد أن هذا الصخر هو مصدر تمعدنات البريل في منطقة وادي الجمال ككل. كشفت دراسة الميكروبروب أن الجارنت هو من النوع السبستين وهو غني في مركزة بأكاسيد

الكالسيوم و الماغنسيوم و التيتانيوم و الاثريوم بينما غني في الحواف بأكاسيد الحديد و الألومنيوم و السيليكون. أكسيد المنجنيز يظهر بعض التفاوت في الوفرة. هذا الاختلاف في التركيب من المركز للحافة يرجع إلي اختلاف نسبة الحديد و المنجنيز حيث يزداد المنجنيز في المركز أكثر من الحواف بينما العكس بالنسبة للحديد.

بينت الدراسة الاشعاعية أن صخر الجرانيت الفوق ألمنيومي يحتوي علي يورانيوم بمتوسط ١٩ جزء في المليون ، ومحتوي ثوريوم بمتوسط ٤ جزء في المليون وهذا مؤداه أن هذا الجرانيت من النوع الخصب.